sustainability

MDPI

Article

Contributing to Carbon Neutrality Targets: A Scenario Simulation and Pattern Optimization of Land Use in Shandong Province Based on the PLUS Model

Xiang-Yi Ma [1], Yi-Fan Xu [1], Qian Sun [2], Wen-Jun Liu [1] and Wei Qi [1,*]

[1] College of Resource and Environment, Shandong Agricultural University, Tai'an 271018, China; 2022110201@sdau.edu.cn (X.-Y.M.); xuyf@sdau.edu.cn (Y.-F.X.); 2022110199@sdau.edu.cn (W.-J.L.)
[2] College of Information Science and Engineering, Shandong Agricultural University, Tai'an 271018, China; applesq@sdau.edu.cn
* Correspondence: qiwei@sdau.edu.cn

Abstract: Land use profoundly impacts the sustainable development of the ecological environment. Optimizing land use patterns is a vital approach to mitigate climate change and achieve carbon neutrality. Using Shandong Province as a case study, this research evaluates the impacts of land use and land cover change (LUCC) on regional carbon storage and emissions. Employing a coupled PLUS–InVEST–GM(1,1) model, simulations were conducted for scenarios including the natural scenario (NS), cropland protection scenario (CPS), high-speed development scenario (HDS), and low-carbon scenario (LCS), to assess LUCC and changes in carbon storage and emissions from 2030 to 2060 under these scenarios. The findings indicate that due to the expansion of construction land and significant declines in arable and grassland areas, carbon emissions increased by 40,436.44 $\times$ 10^4 t over a 20-year period, while carbon storage decreased by 4881.13 $\times$ 10^4 t. Notably, forests contributed the most to carbon sequestration, while construction land emerged as the primary source of carbon emissions. Simulating four scenarios demonstrates that measures such as protecting cropland, expanding forest, grassland, and aquatic areas, controlling construction land expansion, and promoting intensive development positively affect emission reductions and carbon sequestration in Shandong. These findings underscore the importance of rational planning of land use patterns, which can enhance contributions to carbon neutrality by harmonizing the relationships among cropland protection, ecological conservation, and economic development.

Keywords: carbon neutrality; PLUS model; LUCC; land management; scenario prediction

Citation: Ma, X.-Y.; Xu, Y.-F.; Sun, Q.; Liu, W.-J.; Qi, W. Contributing to Carbon Neutrality Targets: A Scenario Simulation and Pattern Optimization of Land Use in Shandong Province Based on the PLUS Model. *Sustainability* **2024**, *16*, 5180. https://doi.org/10.3390/su16125180

Academic Editor: Shunguang Hu

Received: 10 April 2024
Revised: 2 June 2024
Accepted: 13 June 2024
Published: 18 June 2024

1. Introduction

The continuous increase in carbon dioxide is a significant factor contributing to global climate change. In order to mitigate the ongoing global warming, rising sea levels, and occurrences of extreme weather events, nations worldwide need to take action to address these challenges [1]. Since the signing of the Paris Agreement in 2015, China has actively shouldered the responsibility of global climate governance. It has proposed to peak carbon emissions by 2030 and achieve carbon neutrality by 2060. China's climate policies offer significant potential for realizing the emission reduction targets outlined in the Paris Agreement [2]. The Climate Action Tracker (CAT) believes that China achieving carbon neutrality will provide the greatest contribution to global climate change mitigation efforts [3–5].

Land use patterns are among the most significant ways humans affect the climate. Factors such as economic development and urban expansion have led to the conversion of land that provides ecological functions into construction land. These changes have resulted in issues such as rising temperatures, air pollution, and flood disasters [6]. The Intergovernmental Panel on Climate Change (IPCC) believes that effective land management can

facilitate carbon neutrality and mitigate global climate change [7]. As a country with vast land resources, China's scientific approach to land use management is crucial for achieving global emission reduction and carbon sequestration goals [8].

In order to achieve the goals of the carbon neutrality strategy and promote the development of low-carbon land use, scholars have conducted corresponding research focusing on the impact of LUCC on ecosystem carbon cycling and the analysis of driving factors [9–11]. Lai et al. [12] utilized a LUCC dataset to enable the first assessment of how land management and LUCC changes in China affect ecosystem carbon stocks (ECS). They highlighted the necessity to optimize land use structures to enhance the carbon sequestration capacity. Wang et al. [13] utilized the InVEST model and the logarithmic mean Divisia index (LMDI) model to investigate the driving factors of ECS changes in the Loess Plateau region. They revealed the impacts of both natural and social factors on LUCC and carbon storage variations. Yin et al. [14], building upon their analysis of the impacts of LUCC on ECS, conducted an assessment of how ECS contributes to social sustainable development using an indicator system. They emphasized the contribution of improvements in ecosystem carbon sink services (ECSS) to achieving carbon neutrality. Regarding the research on land use carbon emissions (LUCE), scholars have focused on the analysis of carbon emission intensity and the achievement of carbon peak targets [15]. Zhao et al. [16] conducted calculations on the spatiotemporal distribution of carbon emissions in the Shandong Peninsula urban agglomeration based on LUCC data and characterized the spatial autocorrelation of LUCE at the urban level using Moran's I index. Li et al. [17] utilized a carbon emission model to analyze the intensity zoning of LUCE in Tianjin City, uncovering a positive correlation between the expansion of construction land and the variation in LUCE intensity. Zhang et al. [18] conducted carbon emission accounting at the township level to explore the spatial patterns of carbon emissions at a micro-scale level, aiming to assist cities in implementing refined governance. Overall, current research mainly focuses on improving ECS through land use or calculating carbon emission intensity at spatial scales. Few studies have quantitatively analyzed both. In fact, the impact of land use change on carbon stock and carbon emission is simultaneous, and their changes are correlated. Therefore, it is necessary to unify the calculation of LUCE and ECS to evaluate the impact of LUCC on ecosystem carbon cycling. Additionally, due to the inability to directly obtain future regional LUCE data, most studies use historical average values or predictions through exponential smoothing under natural contexts, with fewer studies combining LUCE mathematical prediction models with LUCC simulations [19]. This study couples the GM(1,1) with traditional carbon emission models, effectively improving the accuracy of future carbon emission forecasts.

Future land use changes will have a significant impact on the ecosystem's carbon cycle [20]. With the development of LUCC prediction research, exploring the changes in carbon storage and carbon emissions under future scenarios to seek reasonable land use patterns has become a new research focus [21]. Currently, commonly used models for predicting future land use include the CA-Markov model [22,23], the FLUS model [24], the CLUE-S model [25], and the PLUS model developed by Liang et al. [26]. Some scholars also recognize that, under the influence of various uncertainties in the future, different scenarios of land use may emerge. Wei et al. [27] set up a rural revitalization scenario (RPS) and water–energy–food scenario (WEF) to predict future ECS. Zhang et al. [28] conducted research on the future changes in LUCE under scenarios of farmland protection and low-carbon development. Wang et al. [29] combined the shared socioeconomic pathways and representative concentration pathways (SSP-RCP) to further enhance the feasibility of rational land use management and control. Overall, current research tends to focus more on evaluating LUCC under constant driving factors, overlooking the influence of policy needs and the characteristics of land use in the study area on future LUCC changes [30]. Compared to traditional prediction models, the PLUS model used in this study provides higher LUCC simulation accuracy at the Shandong Province scale. By adjusting the weights and parameters of the driving factors, it can better adapt to the land use change characteristics of different regions and evaluate land use changes under various scenarios.

This study aims to predict the future LUCC in Shandong Province under different policy scenarios, optimizing land use patterns to enhance the contribution towards the regional carbon neutrality goal. Firstly, an analysis of LUCC from 2000 to 2020 in the study area is conducted using a land use transfer matrix, and the spatiotemporal variations of LUCE and ECS are calculated. Subsequently, the PLUS model is employed to forecast LUCC under four scenarios (NS, CPS, HDS, and LCS) for the years 2030 and 2060. Additionally, the GM(1,1) and InVEST models are utilized to evaluate changes in LUCE and ECS for the two periods. Finally, by integrating the research findings with carbon neutrality planning, as well as development plans and policy directions of Shandong Province, recommendations are provided for optimizing land use patterns.

2. Materials and Methods

2.1. Study Area

Shandong Province (114°50′19″–122°42′28″ E, 34°22′15″–38°23′23″ N) is located in the eastern coastal region of China (Figure 1). The terrain is characterized by plains and hills, with mountainous areas protruding in the central and southern parts, low-lying flatlands in the southwest and northwest, and undulating hills in the eastern Shandong Peninsula. The western and northern parts belong to the North China Plain. The province spans the Yellow, Huai, and Hai river systems. The climate is classified as a warm temperate monsoon climate, with annual average temperatures ranging from 11 to 13 °C and average annual precipitation ranging from 550 to 950 mm. As of 2023, the total population of Shandong Province reached 102 million, ranking second in the nation, and its GDP reached 9.2069 trillion yuan, ranking third nationwide. As a major province in heavy industries, Shandong's carbon dioxide emissions rank first in the country. The presence of high-energy-consuming industries and the traditional energy structure increase the difficulty of achieving carbon neutrality. With the implementation of the Shandong Province Spatial Planning (2021–2035), how to achieve the strategic goal of carbon neutrality through optimizing land use structures is an urgent issue for Shandong Province. Utilizing multi-scenario simulations to predict carbon emissions and carbon storage under different scenarios is of great significance for low-carbon land use management and sustainable development.

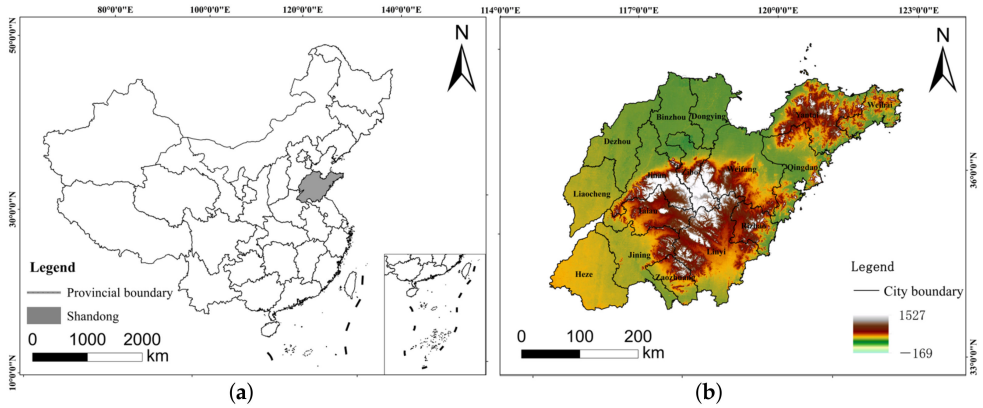

Figure 1. Location of study area. (**a**) Location of the study area in China; (**b**) elevation of the study area.

2.2. Data Sources and Processing

The land cover data from 2000 to 2020 were sourced from the 30 m resolution annual China Land Cover Dataset (CLCD) based on Landsat, produced by Wuhan University on the Google Earth Engine (GEE) platform. This study selected the CLCD data from the years 2000, 2010, and 2020 as the foundational data for evaluating carbon stocks, carbon emissions, and future LUCC dynamic changes (Table 1). Considering that LUCC changes result from the interaction of multiple driving factors, in this study, based on the work of Liang et al. [26], 12 significant factors influencing LUCC were selected from among climate and environmental drivers as well as socioeconomic drivers [31]. The annual average

precipitation and temperature data were sourced from the European Centre for Medium-Range Weather Forecasts (ECMWF). The slope and aspect were derived from the DEM data of NASA's 30 m SRTM dataset. Accessibility data were obtained from Open Street Map and spatially analyzed using Euclidean distance calculations. GDP data were sourced from the Resource and Environmental Science Data Center of the Chinese Academy of Sciences. Population data were obtained from the LandScan data of the Oak Ridge National Laboratory in the United States. Energy consumption data for the study area were sourced from the China Energy Statistical Yearbook. After preprocessing the data, the coordinate systems were unified, and the raster data spatial resolution was uniformly resampled to 100 m.

Table 1. Data sources and specifications.

Data	Attribute	Year(s)	Spatial Resolution	Source
LUCC data		2000, 2010, 2020	30 m	https://zenodo.org/records/5816591 (accessed on 15 November 2023)
Climate	Average annual temperature	2020	1 km	https://cds.climate.copernicus.eu/ (accessed on 7 November 2023)
	Average annual precipitation			
Terrain	SRTM-DEM	2020	30 m	http://srtm.csi.cgiar.org/srtmdata/ (accessed on 15 December 2023)
	Slope			
	Aspect			
Distance	Highway distribution	2020	data	https://www.openstreetmap.org/ (accessed on 7 December 2023)
	Railway distribution			
	Mainway distribution		data	
	River distribution			
Social and economic	GDP	2020	1 km	https://www.resdc.cn/ (accessed on 11 December 2023)
	Population			https://landscan.ornl.gov/ (accessed on 11 December 2023)

2.3. Research Methods

The research framework of this study is illustrated in Figure 2 below. Firstly, based on the LUCC data from 2000 to 2020, we analyzed the land use changes in Shandong Province using the land use transfer matrix (LUTM). Then, we conducted spatial and temporal analyses of LUCE and ECS for this time series separately using carbon emission models and the InVEST model. We incorporated driving factors and the LUCC data into the PLUS model to simulate land use for the years 2030 and 2060 under four scenarios and evaluated LUCE and ECS under different scenarios, wherein the future carbon emission coefficient of construction land is estimated using the grey prediction model GM(1,1). Finally, the simulation results under various scenarios are analyzed. Guided by carbon neutrality goals and benchmarking against Shandong Province's policies on cropland protection and ecological conservation, regional land use and management are optimized.

2.3.1. Analysis of Land Use Change

The land use transition matrix (LUTM) is an application of Markov models in the context of land use change. It quantitatively analyzes the transition states and transition rates between different land use types, aiming to characterize the quantitative changes in the conversion of various land use types. The expression is as follows [32]:

$$S_{ij} = \begin{bmatrix} S_{11} & \cdots & S_{1n} \\ \vdots & \ddots & \vdots \\ S_{n1} & \cdots & S_{nn} \end{bmatrix} \quad (1)$$

where S_{ij} means the land use transition matrix; i means the area of land use types at the beginning of the study period; j means the area of land use types at the end of the study period; and n is the number of land use types.

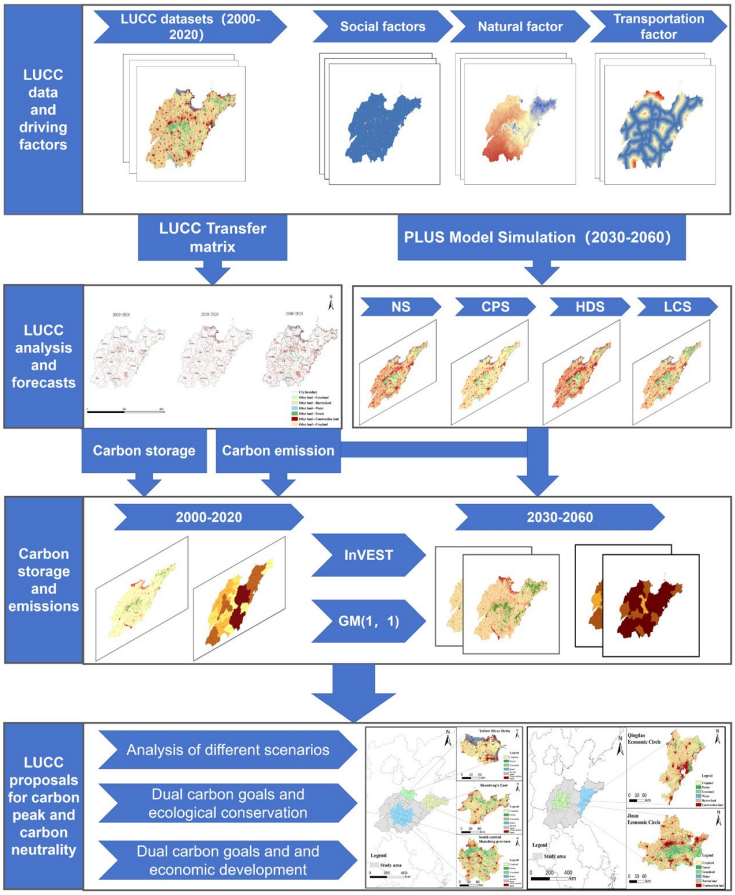

Figure 2. Research framework of this study.

2.3.2. Calculation of Land Use Carbon Emissions

The carbon emissions resulting from land use are defined as direct carbon emissions and indirect carbon emissions [29]. Direct carbon emissions primarily stem from agricultural production, biological respiration, and soil organic matter decomposition activities occurring in cropland, forest, grassland, water, and barren land. Direct carbon emissions can be directly calculated using carbon emission coefficients. The calculation formula is as follows [17]:

$$C_i = \sum S_i \times \theta_i \quad (2)$$

where C_i is the total direct carbon emissions; S_i is the area of land use types; and θ_i is the carbon emission factor for land use types. Based on previous studies, we determined the direct carbon emission factors for different site types (Table 2).

Table 2. Carbon emission factors for land use types.

Types	Carbon Emission Coefficient ($kg \cdot m^{-2} \cdot a^{-1}$)	Source
Cropland	0.0422	[33]
Forest	−0.0644	[16]
Grassland	−0.0021	[34]
Water	−0.0253	[16]
Barren land	−0.0005	[34]

Indirect carbon emissions refer to the carbon emissions generated by human activities in construction land. Due to the uncertainty of human activities, indirect carbon emissions cannot be characterized by a uniform carbon emission coefficient. The combustion of fossil fuels is the primary source of carbon emissions in construction land. Therefore, we calculate the carbon emissions from construction land based on fossil fuel consumption data [35]. The calculation formula is as follows:

$$E = \sum \mathrm{e_i} = \sum E_i \times A_i \times P_i \quad (3)$$

where E means the total carbon emissions from construction land; e_i means total fossil energy consumption; E_i means the carbon emissions from a single fossil energy source; A_i means the standard coal coefficient for type i of fossil fuel; and P_i means the carbon emission coefficient for type i of fossil fuel.

This study identified the primary types of energy consumption in the research area based on the Statistical Yearbook of Shandong Province. These include coal, coke, crude oil, gasoline, kerosene, diesel oil, fuel oil, natural gas, and electricity, totaling nine types of energy. Standard coal coefficients were obtained from the China Energy Statistical Yearbook (2022), and carbon emission coefficients for various types of energy were obtained from the IPCC National Greenhouse Gas Inventories Program (NGGIP) guidelines (Table 3).

Table 3. Standard coal coefficient and carbon emission coefficient for fossil energy.

Types	Standard Coal Coefficient ($kgce \cdot kg^{-1}$)	Carbon Emission Coefficient ($kg \cdot kgce^{-1}$)
Coal	0.7143	0.7559
Coke	0.9714	0.8550
Crude oil	1.4286	0.5857
Gasoline	1.4714	0.5538
Kerosene	1.4714	0.5714
Diesel oil	1.4571	0.5921
Fuel oil	1.4286	0.6185
Electrical power	0.1229	0.7935
Natural gas	1.2143	0.4483

2.3.3. Calculation of Ecosystem Carbon Stocks

In this study, ECS is derived from the InVEST model's carbon module. This model categorizes each land use type into four fundamental carbon pools: aboveground carbon storage, belowground carbon storage, soil organic carbon storage, and dead organic carbon storage [36]. The specific formula for calculating carbon stocks is as follows:

$$C = \sum_{i=1}^{n=6} S(C_a + C_b + C_s + C_d) \quad (4)$$

where C is the total carbon stock; n is the number of land use types; i is an individual land use type; S is the area of the land use type; C_a is aboveground carbon stock; C_b is belowground carbon stock; C_s is soil organic carbon stock; and C_d is dead organic carbon stock.

The carbon density data for this study, which are shown in Table 4, were obtained by selecting regions with the same or similar geographical location to Shandong Province as references. Relevant research findings in these areas were reviewed, and the carbon density was adjusted using climate factors such as annual precipitation and average annual temperature [19,37–39].

Table 4. Carbon intensity of land use types.

Types	C-Above	C-Below	C-Soil	C-Dead
Cropland	33.43	3.34	107.31	0.00
Forest	101.49	26.61	146.41	13.49
Grassland	5.27	21.70	67.71	1.59
Water	10.28	0.00	19.82	0.00
Barren land	40.84	63.73	26.14	0.00
Construction land	34.15	20.24	48.71	0.00

2.3.4. Grey Prediction Model

The grey prediction model GM(1,1) is a method used for forecasting systems containing uncertain factors. Due to the unavailability of carbon emission coefficients for construction land in 2030 and 2060, this study relies on carbon emission data from 2000 to 2020. The GM(1,1) model is employed to predict carbon emissions for 2030, serving as future carbon emission coefficients for construction land [40]. The formula is as follows:

The original series is first accumulated, where the original series is expressed as follows:

$$X^{(0)} = \left[X^{(0)}(1), X^{(0)}(2), X^{(0)}(3), \ldots X^{(0)}(n)\right] \tag{5}$$

A single summation of this original series yields the result:

$$X^{(1)} = \left[X^{(0)}(1), X^{(1)}(2), X^{(1)}(3), \ldots X^{(1)}(n)\right] \tag{6}$$

Derive the formula:

$$X^{(1)}(k) = \sum_{i=1}^{k} X^{(0)}(i) \quad k = 1, 2, 3, \ldots, n \tag{7}$$

Obtain the immediate neighborhood mean generating sequence:

$$z^{(1)} = \left[z^{(1)}(2), z^{(1)}(3), z^{(1)}(4), \ldots z^{(1)}(n)\right] \tag{8}$$

Derive the formula:

$$z^{(1)}(k) = \frac{1}{2}(X^{(1)}(k) + X^{(1)}(k-1)) \tag{9}$$

Construct the GM(1,1) basic formula:

$$b = X^{(0)}(k) + az^{(1)}(k) \tag{10}$$

where, a is the development coefficient; and b is the grey action quantity.

To construct the grey prediction matrix, use B and vector Y:

$$B = \begin{bmatrix} -Z^{(1)}(2) & 1 \\ -Z^{(1)}(3) & 1 \\ \vdots & \vdots \\ -Z^{(1)}(n) & 1 \end{bmatrix} \tag{11}$$

$$Y = \begin{bmatrix} X^{(0)}(2) \\ X^{(0)}(3) \\ \vdots \\ X^{(0)}(n) \end{bmatrix} \tag{12}$$

We assume the following:

$$\hat{a} = [a, b]T \tag{13}$$

The formula obtained for grey differential equations using the method of least squares is as follows:

$$\hat{a} = [a, b]T = \left(B^T B\right)^{-1} B^T Y \tag{14}$$

The whitening equation for the GM(1,1) differential equation can be expressed as follows:

$$b = \frac{dx^{(1)}}{dt} + ax^{(1)} \tag{15}$$

where x is the state variable; t is the time; **a** is the development coefficient; and b is the grey action quantity.

The time response function of the whitening equation is as follows:

$$\hat{x}^{(1)}(k+1) = (X^{(1)}(0) - \frac{b}{a})e^{-ak} + \frac{b}{a} \tag{16}$$

where, K = 0, 1, 2 . . ., n − 1.

The formula for restoring the predicted values is as follows:

$$\hat{x}^{(0)}(k+1) = \hat{x}^{(1)}(k+1) - \hat{x}^{(1)}(k) = (x^{(0)}(1) - \frac{b}{a})(1 - e^{a})e^{-ak} \tag{17}$$

2.3.5. PLUS Model

Liang et al. [26] proposed a rule-mining framework based on the land expansion analysis strategy (LEAS) and a cellular automata (CA) model based on multi-type random patch seeds (CARS). By combining LEAS and CARS, they constructed the patch-based land use simulation (PLUS) model for generating land use simulations. This model can be utilized to simulate changes in land use patches and to explore potential driving factors behind land expansion and landscape changes. It demonstrates the contribution of each driving factor to LUCC. The model offers higher precision simulations compared to other traditional simulation models, enabling the generation of more realistic landscape patterns to support land use decision-making.

In this study, the driving factors are categorized into natural factors, socioeconomic factors, soil factors, and accessibility factors. Using the random forest classification (RFC) algorithm, this study explores the expansion of various land use types and their driving factors (Table 5).

Table 5. Driving Factor Contributions.

Contribution	Cropland	Forest	Grassland	Water	Barren Land	Construction Land
Aspect	0.034	0.058	0.036	0.029	0.067	0.036
DEM	0.123	0.197	0.235	0.123	0.062	0.134
Slope	0.120	0.170	0.107	0.077	0.056	0.132
GDP	0.116	0.059	0.075	0.168	0.096	0.133
Pop	0.067	0.072	0.084	0.179	0.317	0.129
Prec	0.090	0.095	0.066	0.078	0.088	0.056
Temp	0.198	0.127	0.091	0.080	0.079	0.134
River	0.072	0.061	0.082	0.064	0.034	0.069
Railway	0.052	0.044	0.072	0.055	0.052	0.037
Highway	0.040	0.040	0.060	0.051	0.051	0.040
Nationalway	0.042	0.039	0.054	0.045	0.060	0.047
Mainway	0.045	0.037	0.038	0.051	0.037	0.054

Through further screening, the research selected 12 driving factors with a higher contribution (>0.03), including natural factors such as DEM, aspect, slope, annual average temperature, and annual average precipitation; socioeconomic factors such as GDP and population density; and accessibility factors such as distance to rivers, distance to

railways, distance to highways, distance to national roads, and distance to major provincial roads (Figure 3).

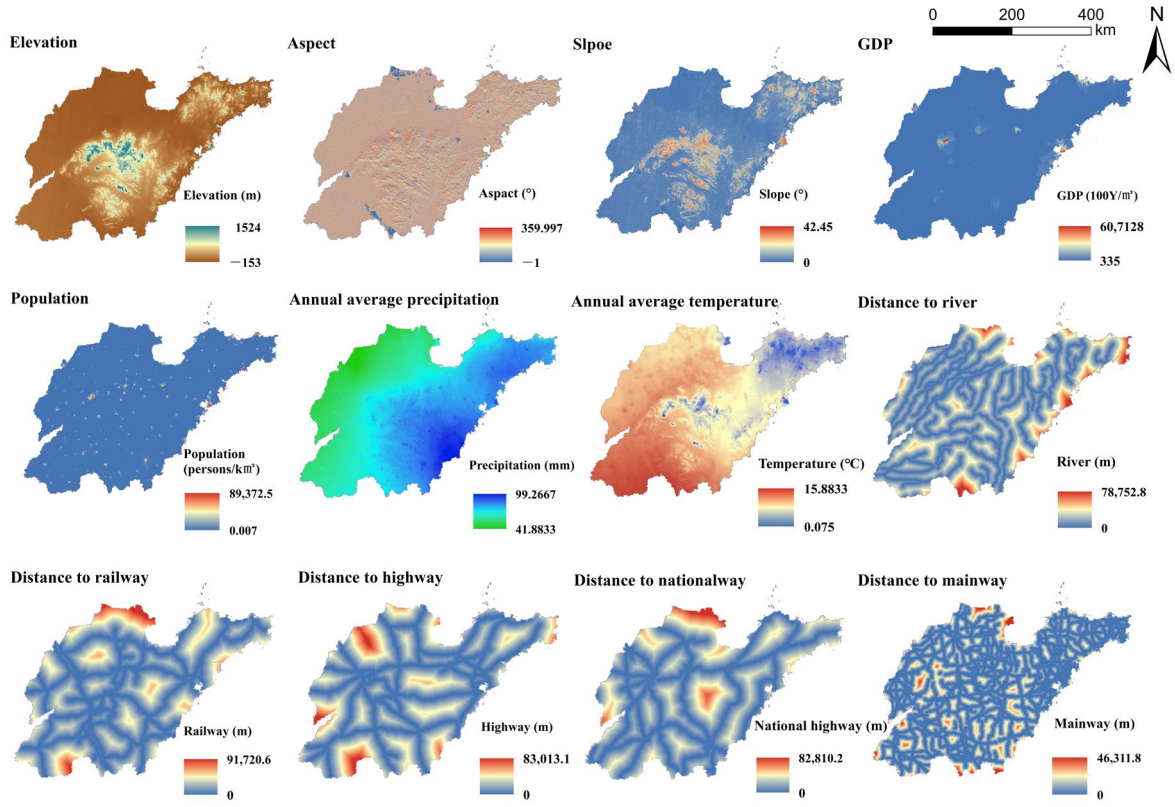

Figure 3. The driving factors influencing LUCC.

Based on the development needs and policy constraints of Shandong Province, we established four different land use scenarios for the years 2030 and 2060.

Natural Scenario (NS): This scenario assumes a business-as-usual situation where there are no significant policy interventions. The land use transition probabilities from 2020 to 2060 remain consistent with those from 2000 to 2020, as predicted by Markov chains. There are no restrictions imposed on the transition of land use types.

Cropland Protection Scenario (CPS): In this scenario, we adhere to the cropland protection targets outlined in the Land Spatial Planning of Shandong Province (2021–2035), aiming to limit the reduction in cropland to no more than 2% every 15 years. There are strict restrictions on the conversion of cropland to other land use types, and reasonable control over the transition between cropland and construction land. Additionally, due to policies such as returning cropland to forests and the balance between cropland occupation and compensation, areas such as forests, grassland, and water that encroach upon cropland require compensatory measures to replenish cropland. Therefore, we allow for a slight conversion of three land use types to cropland.

High-Speed Development Scenario (HDS): In this scenario, economic development is set as the objective for Shandong Province. It involves expanding the central urban areas and satellite city clusters to drive the development of the provincial capital economic zone, the southern Shandong region, the Qingdao metropolitan area, and the Bohai Rim economic zone. The probability of conversion from other land use types to construction land increases, while the conversion of construction land to other land use types is restricted.

Low-Carbon Scenario (LCS): This scenario takes into account the multiple policies and practical needs related to urban development, ecological conservation, and cropland protection. It emphasizes harnessing the carbon sequestration function of ecological land while restricting the conversion of forest, grassland, and water areas to other land use types. Urban expansion is effectively constrained, and efforts are made to optimize the internal

structure of built-up areas, accompanied by improvements in the efficiency of construction land use and upgrades in energy structure. In ecologically protected areas and similar regions, policies such as the conversion of cropland to forests are still being implemented. Additionally, it is essential to consider the persistent policy of cropland protection. While increasing the probability of conversion from the three types of ecological land to other land use types, the reduction in cropland is reasonably controlled. The scenario targets carbon neutrality.

3. Results

3.1. Analysis of Spatial and Temporal Changes in Land Use

The land use transfer Sankey diagram (Figure 4) illustrates the characteristics of land use changes in the research area over a period of 20 years. During the period from 2000 to 2010, cropland primarily shifted towards construction land and water, accounting for a total outflow of 86.78%. The rapid urbanization and urgent economic development needs have led to continuous reduction in cropland areas. Despite the existence of ecological fallow policies, there was still a net inflow of 204.09 km^2 from forests to cropland. From 2010 to 2020, the effectiveness of ecological protection policies became apparent. The change in forest areas shifted from a decrease to an increase. Under strict policies of converting forests to cropland, there was a transfer of 1262.02 km^2 from cropland to forests, accounting for 63.75% of the total increase in forest areas. The cropland outflow was more severe during this period, with a transfer of 5711.04 km^2 to construction land, constituting 71.49% of the total outflow. The inflow of cropland primarily came from forest, grassland, and water areas, reaching 478.84 km^2, 876.48 km^2, and 660.84 km^2, respectively. This is mainly attributed to the land balance policy for farmland in Shandong Province. Due to the expansion plans of construction land in the Yellow River Delta region and the requirements for the construction of water conservancy facilities across the province, the outflow of water to construction land reached 390.69 km^2.

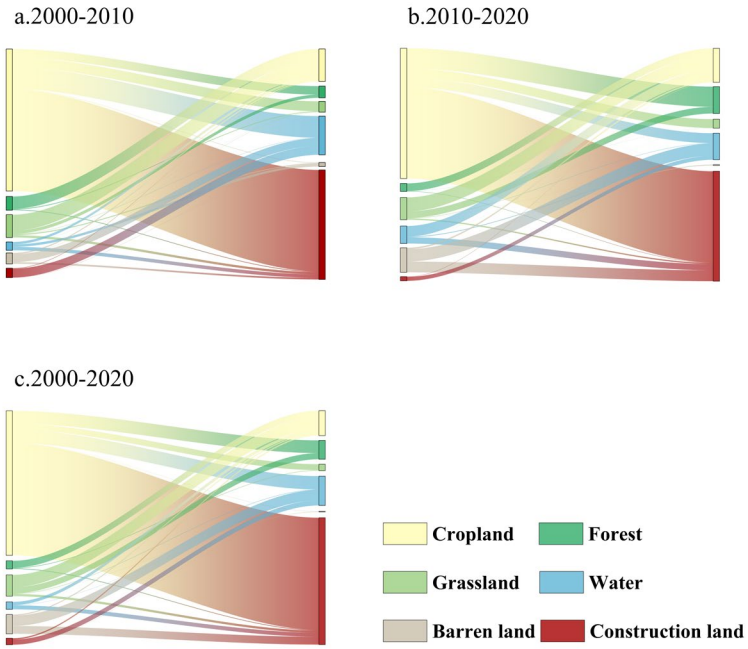

Figure 4. Sankey diagram of land use change from 2000 to 2020.

The LUTM (Table 6) illustrates the changes in quantities among different land types over a period of 20 years. Overall, despite a significant outflow of cropland to construction land totaling 11,114 km^2 from 2000 to 2020, cropland remained the predominant land type in the research area. Approximately 67.38% of the total increase in forests came from cropland. Grassland predominantly flowed out to cropland and forests, accounting for 58.35% and

28.85% of the total outflow, respectively. Water increased by a total of 2169.72 km^2, replacing grassland as the fourth-largest land use type. Unused land primarily transferred to water (53.97%) and construction land (40.42%). Over the 20-year period, urbanization in Shandong Province continued to advance, with a significant expansion of construction land, showing a continuous growth trend, totaling an increase of 11,925.05 km^2, representing a growth rate of 52.17%.

Table 6. Land use transfer matrix 2000–2020 (Unit: km^2).

Type	Cropland	Forest	Grassland	Water	Barren Land	Construction Land	Total
Cropland	103,554.57	1259.28	587.10	1330.28	20.78	11,114.00	117,866.01
Forest	689.83	5955.26	48.20	0.76	0.11	63.75	6757.91
Grassland	1229.14	607.66	1562.24	39.27	11.22	219.12	3668.65
Water	316.87	1.56	0.45	2345.56	18.58	399.65	3082.67
Barren land	106.10	0.00	1.10	1031.38	224.15	772.47	2135.20
Construction land	131.18	0.37	0.08	505.14	7.17	22,214.44	22,858.38
Total	106,027.69	7824.13	2199.17	5252.39	282.01	34,783.43	156,368.82

Figure 5 illustrates the spatial changes in land use from 2000 to 2020. In accordance with the requirements outlined in the "Land Spatial Planning of Shandong Province 2006–2020", forests and grassland have been concentrated in Central-South Shandong and East Shandong. The expansion of water primarily focuses on the Yellow River Delta in the northern part of Shandong, owing to stringent government policies on ecological conservation and scientific development in this region. Within this area, there has also been a shift in water towards construction land, indicating a parallel expansion of construction land and ecological conservation policies. The changes in construction land in the study area align with the demands of the "New Urban Planning of Shandong Province (2014–2020)", with significant expansion observed in the core urban agglomerations of Jinan and Qingdao, as well as in the Yellow River Delta Economic Development Zone and the urban development areas in southern Shandong.

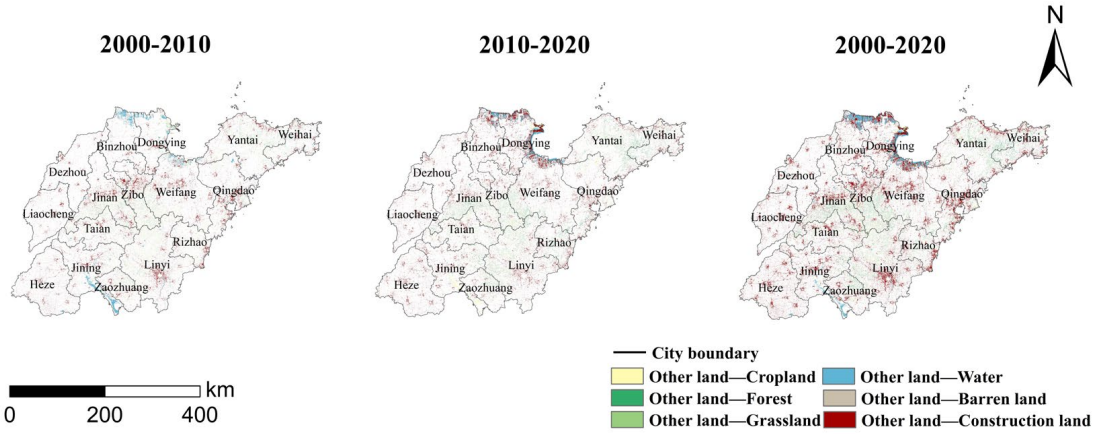

Figure 5. Map of land use transfer 2000–2020.

3.2. Spatial and Temporal Variations in Carbon Stocks and Emissions from Land Use

3.2.1. Changes in Ecosystem Carbon Stocks

This study assessed the changes in ECS in Shandong Province from 2000 to 2020. The results indicate (Table 7) that the total ECS decreased by 2.22% over the 20-year period, totaling 4881.13 × 10^4 t. Among these, the ECS reduction in cropland accounted for 81.62% of the total decrease, amounting to a reduction of 17,047.18 × 10^4 t. Carbon stocks notably increased in construction land and forests, with construction land increasing by 12,282.80 × 10^4 t. Forests exhibited a fluctuating pattern of decrease and subsequent increase over the 20 years, proportional to changes in forest area, resulting in a total increase of 3070.71 × 10^4 t. According to carbon pool data, both above ground carbon stocks and

soil organic carbon are identified as the primary sources contributing to ECS among various land use types.

Table 7. Carbon stock changes 2000–2020 (Unit: 1×10^4 t).

Types	2000–2010		2010–2020		2000–2020	
	ECS	Rate	ECS	Rate	ECS	Rate
Cropland	−8365.95	−4.93%	−8681.23	−5.38%	−17,047.18	−10.04%
Forest	−311.01	−1.60%	3381.72	17.66%	3070.71	15.78%
Grassland	−609.12	−17.30%	−801.58	−27.52%	−1410.70	−40.06%
Water	482.50	52.17%	168.42	11.97%	650.92	70.38%
Barren land	−480.97	−17.20%	−1946.71	−84.05%	−2427.68	−86.79%
Construction land	5470.34	23.23%	6812.46	23.48%	12,282.80	52.17%
Total	−3814.22	−1.73%	−1066.91	−0.49%	−4881.13	−2.22%

Figure 6 depicts the spatial characteristics of ECS over the past 20 years. The results indicate that high carbon stocks are primarily concentrated in the central region and the eastern peninsula of Shandong Province. These areas are characterized by large contiguous forest areas, which largely correspond to the ecological barriers of the Central and Southern Shandong mountainous and hilly ecological barrier and the Eastern Shandong low mountainous and hilly ecological barrier regions designated in the ecological restoration plan of Shandong Province. Carbon stocks in the Yellow River Delta region experienced a significant decrease over the 20-year period. Overall, influenced by the development plans in the Yellow River Delta region, the decrease in carbon stocks is mainly attributed to cropland, while the increase in carbon stocks mainly comes from water and construction land.

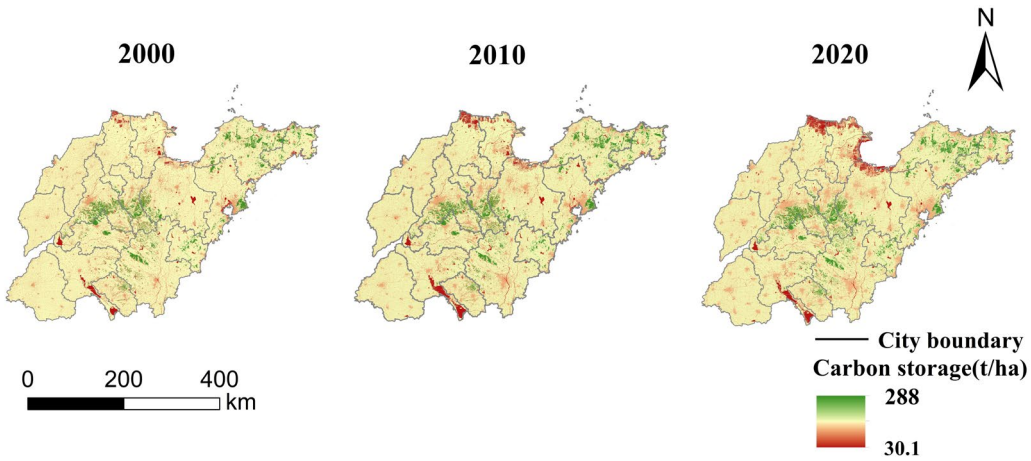

Figure 6. Map of carbon stock changes 2000–2020.

3.2.2. Changes in Carbon Emissions from Land Use

Table 8 presents the changes in LUCE from 2000 to 2020. The results indicate that over the 20-year period, total carbon emissions increased from 8772.04 $\times 10^4$ t to 49,208.48 $\times 10^4$ t. Construction land contributed the most to the growth in carbon emissions, increasing from 8326.84 $\times 10^4$ t to 48,825.19 $\times 10^4$ t. These figures represent 94.92%, 98.78%, and 99.22% of Shandong Province's total carbon emissions for the years 2000, 2010, and 2020, respectively. Forests served as the primary carbon sink, with carbon sequestration reaching 50.39 $\times 10^4$ t by 2020, reflecting a 15.79% increase compared to 2000.

This study classified the carbon emission intensity of various prefecture-level cities in Shandong Province into five levels using the natural breakpoint method. These levels are as follows: low emission (<913.86 $\times 10^4$ t), relatively low emission (913.87–1932.89 $\times 10^4$ t), moderate emission (1932.90–3015.95 $\times 10^4$ t), relatively high emission (3015.96–4635.92 $\times 10^4$ t), and high emission (>4635.93 $\times 10^4$ t). Figure 7 illustrates the changes in carbon emission intensity and total emissions over the past two decades. The increase in carbon emissions

is concentrated in the eastern and southern regions of the study area. As key cities for industrial and agricultural development, Weifang and Linyi have reached high levels of carbon emission intensity. Although carbon emissions from construction land in the Jinan and Qingdao metropolitan areas have increased, the presence of the Eastern Shandong Ecological Protection Zone and contiguous forests in the southern mountainous regions has somewhat constrained the overall increase in carbon emissions in these areas. Overall, there is a noticeable increase in carbon emission intensity across prefecture-level cities in Shandong Province, with higher levels observed in the eastern and southern regions and lower levels in the western and northern regions.

Table 8. Carbon emissions changes 2000–2020 (Unit: 1×10^4 t).

Types	2000	2010	2020
Cropland	497.39	472.88	447.44
Forest	−43.52	−42.83	−50.39
Grassland	−0.77	−0.64	−0.46
Water	−7.80	−11.87	−13.29
Barren land	−0.11	−0.09	−0.01
Construction land	8326.84	33,927.99	48,825.19
Total	8772.04	34,345.45	49,208.48

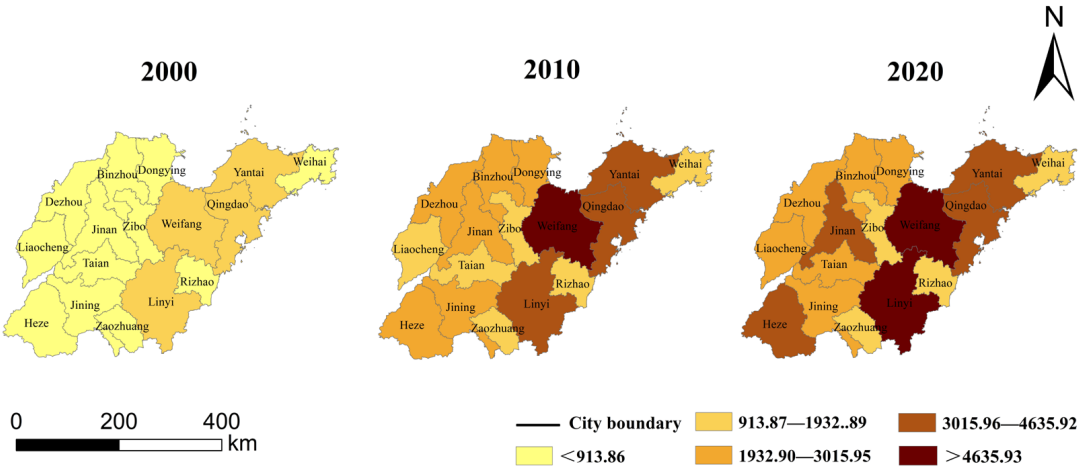

Figure 7. Map of carbon emissions changes 2000–2020.

3.3. PLUS Model Simulations

3.3.1. Land Use Scenario Modelling

Before conducting LUCC simulations using the PLUS model, it is necessary to validate the accuracy of the model [41]. This study conducted LUCC simulations for the year 2020 based on land use data from 2010 using the PLUS model. A comparison with actual LUCC data for 2020 was performed for validation, and the results are presented in Figure 8. The kappa coefficient was found to be 0.7705, with an overall accuracy (OA) of 88.96%. These results demonstrate that the PLUS model exhibits high simulation accuracy, indicating its suitability for land use prediction under various scenarios.

We incorporated driving factors and constraints from different scenarios into the PLUS model to simulate land use patterns for the four scenarios. The results indicate (Table 9) that from 2030 to 2060, there is a decrease in cropland under all four scenarios. The HDS scenario experiences the greatest reduction in cropland, declining from 97,597.69 km^2 in 2030 to 76,229.38 km^2 in 2060, a total decrease of 21.89%. The CPS scenario shows the smallest change in cropland, decreasing by a total of 6626.55 km^2 over the 30-year period. The area of construction land significantly increases under all four scenarios, with the HDS scenario witnessing the most substantial growth from 43,627.73 km^2 in 2030 to 65,386.50 km^2 in 2060, a 49.87% increase. Conversely, expansion of construction land is constrained under

the LCS scenario, with a total growth of 7383.49 km^2. Apart from a reduction of 539.78 km^2 in forests under the CPS scenario, the area of forests increases to varying degrees under the other three scenarios. However, there is a significant decrease in grassland area across all scenarios.

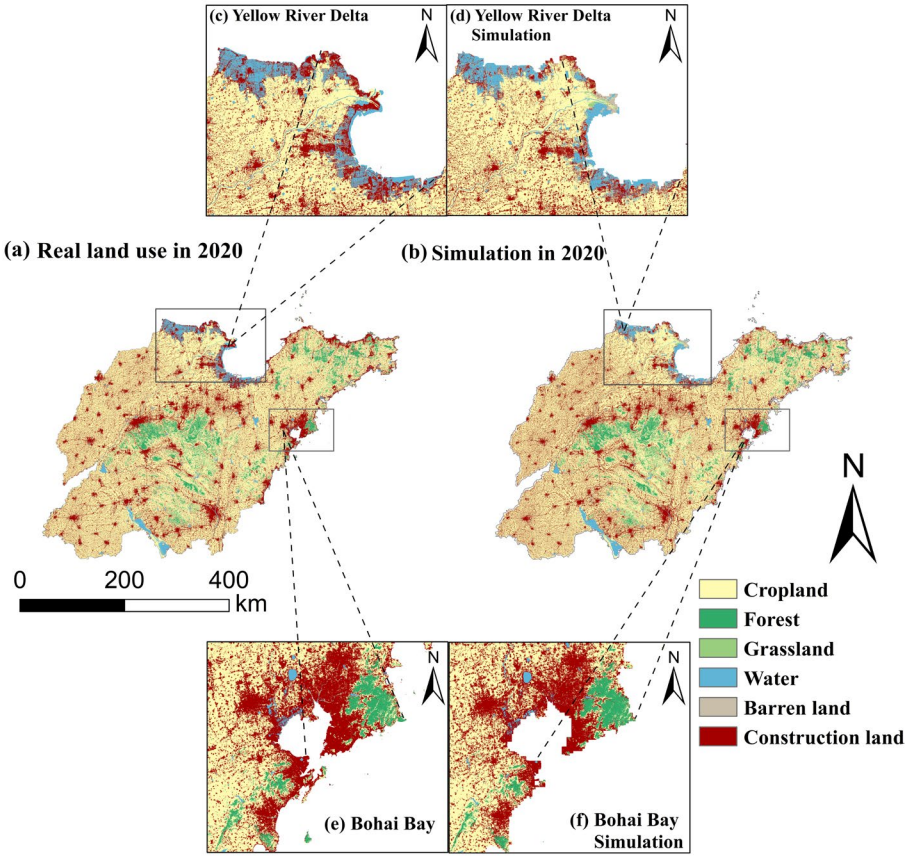

Figure 8. Comparison of land use in 2020. (**a**) Map of current land use in 2020. (**b**) Results of the PLUS model simulation of the current land use situation in 2020. (**c**–**f**) Regional differences in LUCC simulations.

Table 9. Land use area changes under four scenarios 2030–2060 (Unit: km^2).

Type	Cropland	Forest	Grassland	Water	Barren Land	Construction Land
NS2030	100,285.03	8727.00	1718.12	5054.62	94.00	40,490.05
NS2060	84,989.78	10,405.19	1126.35	4553.71	59.06	55,234.73
CPS2030	104,577.00	7788.05	1214.17	4425.58	88.99	38,275.02
CPS2060	97,950.45	7248.27	511.22	3036.61	41.00	47,581.27
HDS2030	97,597.69	8679.02	1688.01	4696.84	79.52	43,627.73
HDS2060	76,229.38	10,066.94	1030.38	3610.45	45.18	65,386.50
LCS2030	101,257.92	9542.60	2146.02	5803.56	71.57	37,547.15
LCS2060	89,158.19	13,671.16	1933.00	6620.90	54.93	44,930.64

Figure 9 illustrates the different land use patterns under four future scenarios. Cropland remains the predominant land use type in Shandong Province, but it consistently decreases over the 30-year period, significantly shifting towards construction land and forests. Construction land under all scenarios expands outward from Jinan and Qingdao, with a noticeable increase in the number of medium-sized and small urban clusters. Changes in forests, grasslands and water are primarily concentrated in the Yellow River Delta region. Changes in forests and grasslands are concentrated in key ecological conservation areas such as the central and southern Shandong mountainous region, Yimeng mountainous region, and eastern Shandong region as outlined in the Shandong Province Ecological Restoration Plan 2021–2035.

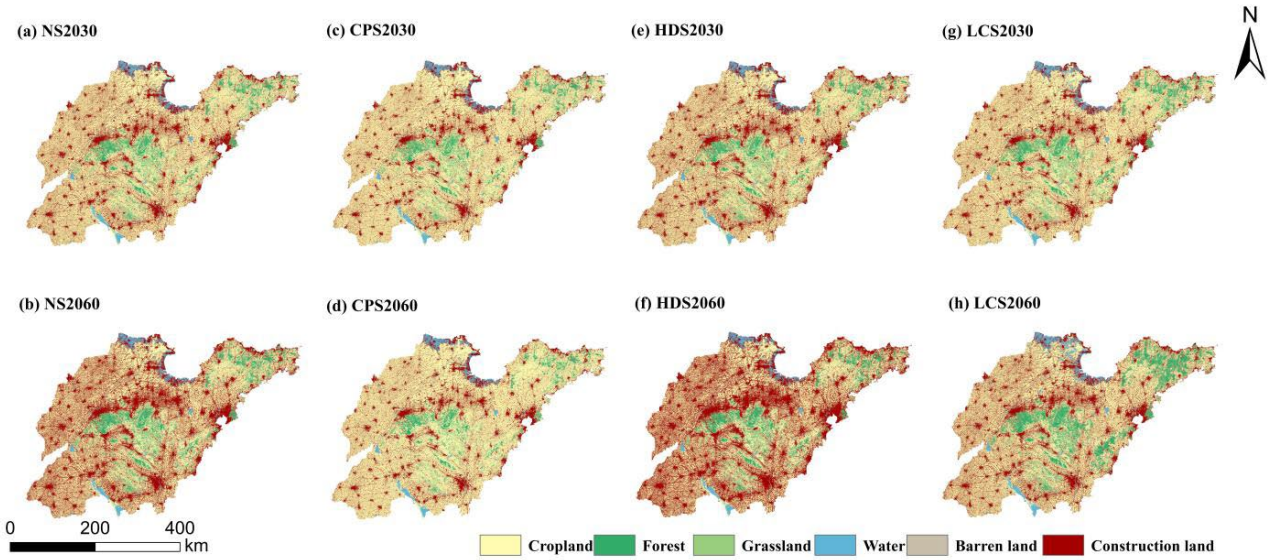

Figure 9. Land use simulation for four scenarios 2030–2060.

3.3.2. Carbon Stock Modelling under Different LUCC Scenarios

This study evaluated the variation in ECS under different LUCC scenarios from 2030 to 2060. The results indicate (Table 10) that compared to 2020, carbon stocks decreased under the NS, CPS, and HDS scenarios. Among these, the HDS scenario experienced the most significant loss in carbon stocks, totaling 6853.99 $\times$ 10^4 t. Under the NS scenario, carbon stocks decreased by 3327.87 $\times$ 10^4 t. The reduction in carbon stocks under the CPS scenario was concentrated between 2030 and 2060, with an average annual decrease in ECS of 0.41%. Conversely, the LCS scenario was the only one where carbon stocks increased, with a total increment of 2856.56 $\times$ 10^4 t from 2020 to 2060, representing an average annual increase of 0.33%.

Table 10. Carbon stock projections for four scenarios (Unit: 1 $\times$ 10^4 t).

Scene	2020–2030		2030–2060		2020–2060	
	ECS	Rate	ECS	Rate	ECS	Rate
NS	−558.78	−0.26%	−2769.10	−1.29%	−3327.87	−1.55%
CPS	−43.04	−0.02%	−2665.77	−1.24%	−2708.81	−1.26%
HDS	−1490.11	−0.69%	−5363.88	−2.51%	−6853.99	−3.19%
LCS	766.01	0.36%	2090.55	0.97%	2856.56	1.33%

According to the research findings (Figure 10), in the NS, CPS, and HDS scenarios, low-carbon storage areas are concentrated in regions where there is a reduction in cropland area and in the Yellow River Delta region. In the LCS scenario, the increase in carbon storage is closely associated with the expansion of forests, while the growth in ECS is concentrated in the eastern Shandong region and the southeastern mountainous areas. The relatively low carbon sequestration capacity in the Yellow River Delta under all four scenarios is attributed to the extensive expansion of water areas in that region. In terms of the ecological and economic development zoning of Shandong Province, areas with high ECS are concentrated in the ecological barrier zones of the central and southern mountainous regions and the low hills of eastern Shandong. Conversely, areas with decreased carbon storage are consistent with changes in construction land and water areas, focusing on the urban areas of Jinan and Qingdao metropolitan circles, as well as the Yellow River Delta water conservation area.

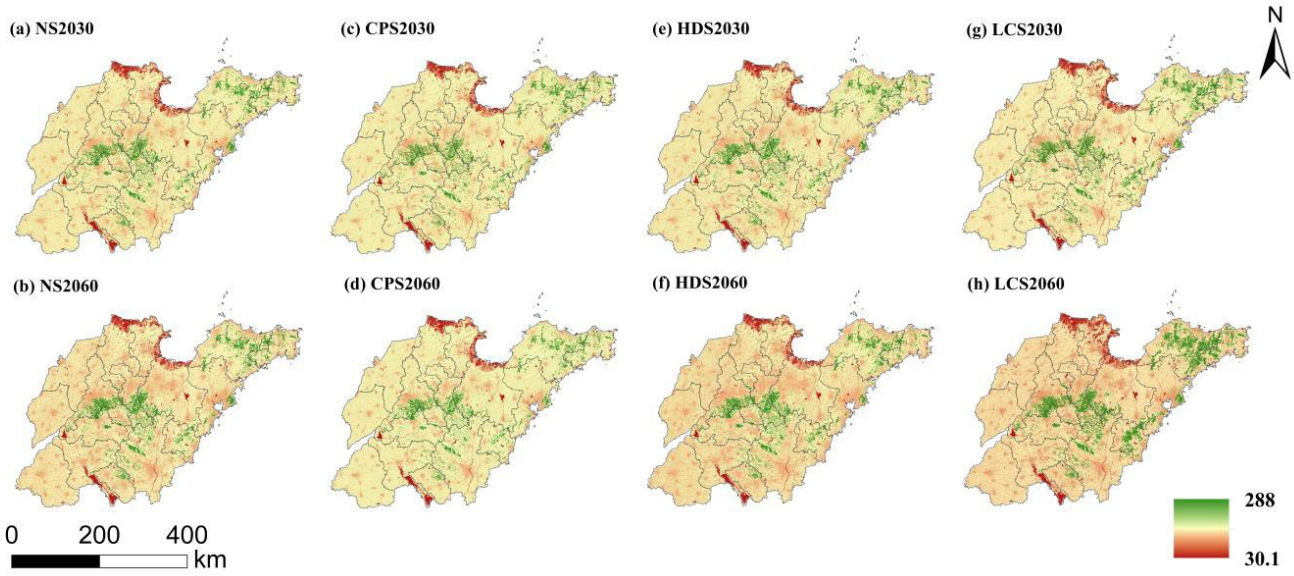

Figure 10. Carbon stocks simulation for four scenarios 2030–2060.

3.3.3. Modelling of Carbon Emissions under Different Scenarios

In the absence of future indirect carbon emission data, we predicted the carbon emission coefficient of construction land after reaching the carbon peak in 2030 using the GM(1,1) model. By calculating energy consumption data and construction land area, we obtained the carbon emission coefficients of construction land for the years 2000, 2010, and 2020, which were 3.643 kg/hm^2, 12.044 kg/hm^2, and 14.037 kg/hm^2, respectively. By applying this information, we obtained a carbon emission coefficient for construction land in 2030 as 16.3150 kg/hm^2. With an average relative error of 1.61%, this confirms the high accuracy of the prediction results. Using this coefficient, we can calculate the total carbon emissions from 2030 to 2060 (Table 11).

Table 11. Carbon emissions projections for four scenarios (Unit: 1×10^4 t).

Scene	2020–2030		2030–2060		2020–2060	
	LUCE	Rate	LUCE	Rate	LUCE	Rate
NS	17,205.05	34.96%	23,982.04	36.11%	41,187.10	83.70%
CPS	13,617.08	27.67%	15,162.37	24.13%	28,779.45	58.48%
HDS	22,314.08	45.35%	35,403.29	49.50%	57,717.36	117.29%
LCS	12,400.56	25.20%	11,966.52	19.42%	24,367.08	49.52%

Overall, carbon emissions continue to increase across all four scenarios, with construction land being the primary source of carbon emissions. Under the HDS scenario, LUCE saw a significant increase of 117.29%, rising from 49,208.48 $\times$ 10^4 t in 2020 to 106,925.84 $\times$ 10^4 t in 2060. Under the LCS scenario, LUCE saw an increase of 49.52% over the 40-year period, reaching a total carbon emission of 73,575.56 $\times$ 10^4 t in 2060. During the period from 2030 to 2060, LUCE only increased by 19.42%, which is significantly lower than the increases observed in the other three scenarios. Under the CPS scenario, carbon emissions increased by a total of 58.48%, over the 40-year period, second only to the LCS scenario. All four scenarios were subject to the carbon peak policy in 2030, resulting in a slowdown in the rate of carbon emissions growth after 2030.

Figure 11 illustrates the spatial variations of carbon emission intensity under the four scenarios. In the NS and CPS scenarios, the carbon emission intensity remains largely consistent, with the increase in emissions primarily concentrated in the northern and southern regions of Shandong Province. By 2060, the carbon emissions across the province

are predominantly at high and relatively high intensity levels. The spatial variations in LUCE align with urban expansion areas. In the HDS scenario, carbon emissions in Shandong Province are mainly at the high intensity level, with only Weihai, Rizhao, Zibo, Liaocheng, and Zaozhuang classified as higher intensity. In the LCS scenario, the high intensity areas in 2030 and 2060 continue to be concentrated in the eastern and southern parts of Shandong, while the central and southern regions benefit from increased forest area, enhancing carbon sequestration capacity and thus mitigating carbon emissions. Overall, high carbon emission areas are consistent across all scenarios. Yantai, Weifang, and Linyi consistently exhibit high intensity levels from 2030 to 2060, while Heze, Jining, Qingdao, and Dezhou also reach high intensity levels by 2060.

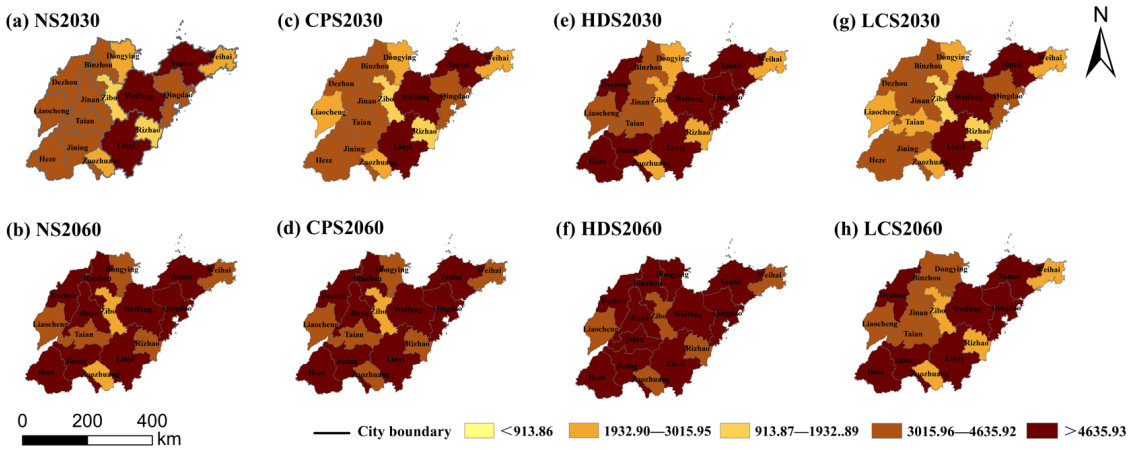

Figure 11. Carbon emissions simulation for four scenarios 2030–2060.

4. Discussion

4.1. Future Carbon Emission and Carbon Stock Affected by LUCC

Effective and sustainable management of land resources is a key initiative for achieving carbon peaks and carbon neutrality [42,43]. This study evaluates LUCE and ECS simultaneously to determine how to optimize land use patterns under the carbon neutrality target. Unlike previous studies that often use the FLUS model or the CLUE-S model [44], the PLUS model used in this study provides higher accuracy in large-scale land use prediction and is applicable to simulation requirements under different scenarios [45,46]. Coupling the InVEST model with the GM(1,1) model allows for a better quantitative assessment of future carbon storage and emissions in the study area. Determining carbon emission intensity at the prefectural level is of great significance for zoning management of land use.

The research findings indicate that changes in carbon stock are largely consistent with changes in land use (Figure 6). In the central and eastern regions of Shandong Province, high carbon storage areas correspond to regions with concentrated forests, while low carbon storage areas correspond to regions with significant increases in water and construction land. For example, the Yellow River Delta region, influenced by regional spatial planning, has seen significant increases in water areas and construction land areas, leading to a corresponding decrease in carbon sequestration capacity. The change in carbon emissions is influenced by changes in the area of construction land and forests. The results show that in regions where carbon emission intensity is rising, there is significant expansion of construction land while forest areas experience notable reduction (Figures 9 and 11). For example, in Weifang and Linyi, key industrial cities in Shandong Province, the urbanization rate reaches 65.2%. However, these areas lack land types such as forests and grasslands, leading to higher carbon emission intensity. The mitigation of carbon emission growth relies on changes in the area of forests, grasslands, and water bodies. For instance, Tai'an in the central-southern region of Shandong and Dongying in the Yellow River Delta region have large areas of forests and water bodies, resulting in significantly lower carbon emission intensity compared to other prefecture-level cities. Overall, the impact of LUCC on LUCE

and ECS in the study area is generally consistent with previous studies [47–49]. The research findings indicate that the increase in carbon storage in the study area primarily stems from cropland, forests, and grassland. In the central-southern and eastern regions of Shandong, extensive forest land serves as the main contributor to ECS. This is largely attributed to the Shandong Province Ecological Barrier Construction Plan. However, cropland and grassland in the study area continue to diminish, resulting in the inability of the increased carbon sink in forest land to offset the decrease in carbon storage. Additionally, due to the rapid economic development and increasing urbanization levels over the 20-year period, the area of construction land in Shandong Province has continuously expanded. Industrial activities, energy consumption, and human activities within construction land are the main sources of carbon emissions [50]. The expansion of urban clusters is directly proportional to the increase in carbon emissions. From 2000 to 2020, the increment in ECS in Shandong Province significantly lagged behind the decrement, while there was a notable increase in LUCE. This has led to significant pressure in Shandong Province for emission reduction and carbon sink enhancement.

4.2. Optimization of Land Use Patterns and Policy Recommendations

After simulating LUCC under four different scenarios, we found significant impacts of different land use types on LUCE and ECS. In the HDS scenario, driven by the need for economic development and substantial population growth, there was an expansion of construction land at the expense of cropland, forests, grassland, and water. This scenario resulted in a substantial increase in carbon emissions. Cropland served as the primary source of expansion for construction land; thus, the cropland protection policy under the CPS scenario had a certain inhibitory effect on construction land expansion, leading to only a slight increase in LUCE compared to the LCS scenario. In the LCS scenario, economic development is no longer the primary concern, and the increase in forest area can offset the carbon emissions generated by the expansion of construction land. In the HDS scenario, there was a notable decrease in carbon sequestration capacity and a significant increase in LUCE. LCS is the only scenario where carbon storage increases, and it also has the lowest carbon emissions. This suggests that achieving carbon neutrality targets by 2030 or even 2060 may be challenging if rapid expansion of construction land continues. Limiting the conversion of cropland to construction land effectively restricts the increase in carbon emissions. Additionally, the growth of ecological land, particularly forests, maximizes carbon sinks. Therefore, we need to consider cropland protection and ecological conservation as management strategies for emission reduction and carbon sink enhancement.

The expansion of construction land is concentrated in the Jinan economic circle and the Qingdao economic circle (Figure 12). The "Shandong Province Land Spatial Planning (2021–2035)" designates the Jinan and Qingdao metropolitan areas as economic centers, with Yantai, Linyi, and Weifang serving as secondary economic centers. This planning is largely consistent with the expansion areas of construction land in our simulation results. Constrained by ecological protection red lines and cropland protection red lines, the Qingdao economic circle chooses to expand around Jiaozhou Bay, while the Jinan economic circle opts for lateral expansion from east to west [51]. The results of the HDS scenario indicate that the expansion of construction land should be subject to a certain degree of restraint and control. Future urban development requires efficient utilization and intensive management of built-up areas [52]. The ongoing implementation of urban–rural integration development in Shandong Province, along with the strict demarcation of the scale and expansion boundaries of urban construction land, represents a significant policy for the efficient utilization of construction land. Such policies play a crucial role in enhancing regional economic development and improving residents' living standards [53]. Construction land is the primary source of carbon, and fossil energy consumption is the main cause of carbon emissions from construction land. Therefore, industrial transformation and green production will be the key to reducing emissions and increasing carbon sinks on urban land in the future [54].

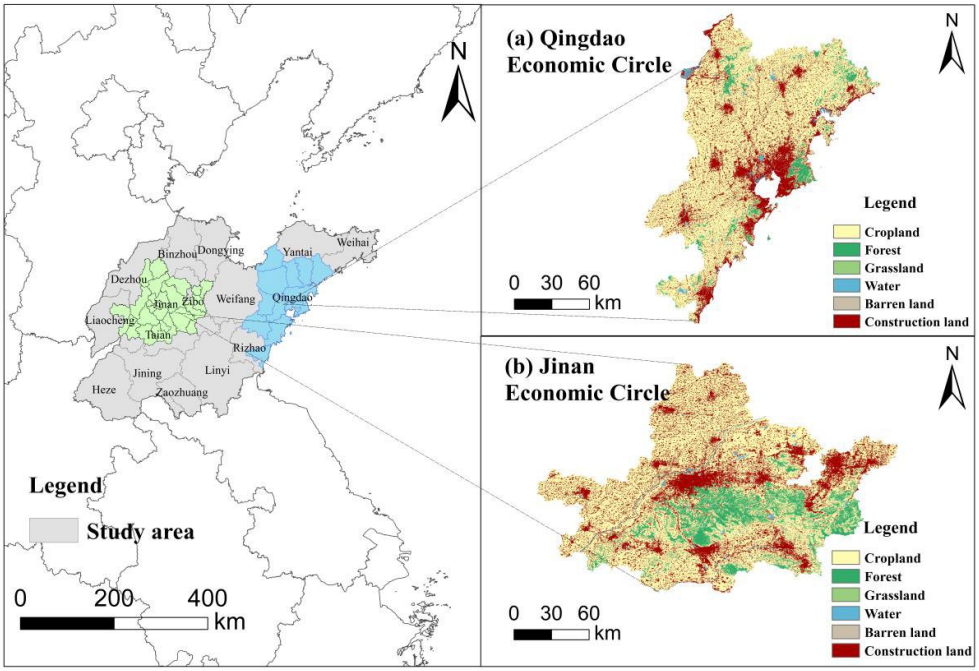

Figure 12. Map of economic circles in Shandong Province.

Shandong Province is a major agricultural production region and a key area for cropland protection in China, ranking third in total grain output nationwide. Considering the positive role of cropland protection in carbon balance under the CPS scenario, it is necessary to ensure the quantity of cropland within the government-designated cropland protection red line. Rational cropping systems and the improvement of cropland quality can increase soil organic carbon reserves [55], thus enhancing cropland's carbon sequestration capacity. Research indicates a decrease in cropland area across all four scenarios, highlighting the need for strict implementation of policies ensuring a balance between the occupation and compensation of cropland. Emphasis should be placed on the restrictive role of cropland protection policies in curbing the expansion of construction land [56].

Research findings indicate that ecological protection efforts in Shandong Province are concentrated in the Yellow River Delta, the hills and low mountains of eastern Shandong, and the hilly areas of south-central Shandong (Figure 13). The ongoing Ecological Restoration Project (ERP) in the Yellow River Delta has demonstrated significant effectiveness [57]. Preservation of biodiversity and enhancement of water conservation capacity in the Yellow River Delta have positive impacts on increasing regional carbon storage [58]. The eastern Shandong region, including the hills and low mountains, constitutes one of the province's two major ecological barriers, boasting extensive natural forests, economic forests, and timber forests. Protecting forested areas in the hills and low mountains of eastern Shandong maximizes the carbon sequestration capacity of forest ecosystems [59,60]. However, this research indicates significant reduction in forest areas in the region under the HDS scenario, highlighting the vulnerability of these forests to policy changes. Therefore, it is essential to continue implementing strict specialized protection measures based on existing ecological conservation plans in order to safeguard these valuable ecosystems. South-central Shandong possesses extensive areas of pristine forests and afforestation land. As the most crucial ecological barrier zone in Shandong Province, there remains a pressing need to significantly increase afforestation areas in mountainous regions. It is imperative to manage the relationship between urban development boundaries and ecological protection red lines effectively. This will not only enhance ecosystem services but also to some extent restrain the unrestricted expansion of the Jinan metropolitan area while improving the ECS.

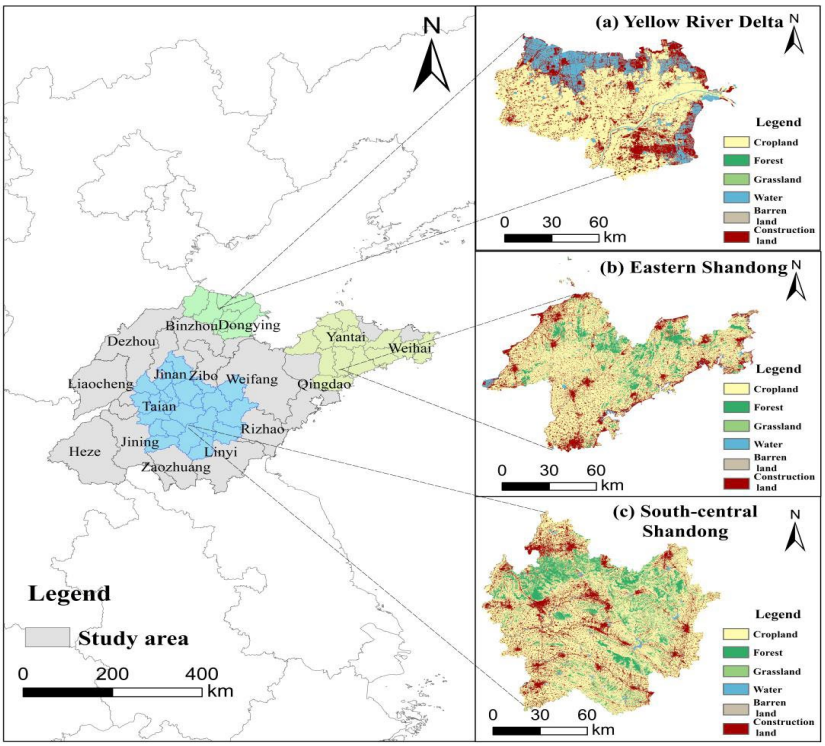

Figure 13. Map of ecological reserves in Shandong Province.

4.3. Research Limitations and Prospects

Our study has several limitations that need to be addressed in future research. Firstly, considering the large extent of the study area, the base data resolution we used is not the highest available, which could impact the accuracy of LUCC predictions. Secondly, the multi-source data used in this study vary in precision and quality, affecting the reliability of the results. In the multi-scenario simulations of land use, the PLUS model's results depend on the setting of model parameters and weight adjustments. The parameters we set are based on historical research and experience, which may lead to errors and lag in different scenario simulations. Additionally, scenario simulations cannot predict the drastic changes brought by natural disasters and policy shifts, resulting in an inability to fully represent the actual land use situation. Lastly, the GM (1,1) model we used is for calculating increasing sequences, providing better accuracy in obtaining future carbon emission coefficients for construction land [61]; it cannot determine the mitigating effects of future industrial upgrades and the use of clean energy on carbon emissions. In future studies, we will explore the impact mechanisms of LUCC coupled with energy structures and soil carbon sinks on LUCE and ECS based on high-resolution datasets. This will enable us to optimize land use patterns more effectively.

5. Conclusions

This study explores the impacts of LUCC on LUCE and ECS. Based on LUCC data and driving factor data, a coupled PLUS–InVEST–GM(1,1) model is used to analyze carbon emissions and carbon storage changes in Shandong Province from 2000 to 2020 and predict four different scenarios for the period 2030 to 2060. Finally, through comparing these scenarios and considering the current spatial planning of Shandong Province, policy recommendations are provided for optimizing land use patterns under the context of carbon neutrality. The results of this study are as follows:

(1) From 2000 to 2020, the maximum reduction in cropland area reached 17,047.18 km^2. There was an increase of 11,925.05 km^2 in construction land. The ECS consistently experienced a reduction, decreasing by a total of 4881.13 $\times$ 10^4 t over the 20-year

period. Forests are the dominant carbon sink. The carbon emissions have shown a year-on-year increase, rising significantly from 8772.04 $\times$ 10^4 t to 49,208.48 $\times$ 10^4 t. The carbon emission intensity of prefecture-level cities has been increasing year by year. Among them, cropland and construction land are the primary sources of carbon emissions.

(2) From 2030 to 2060, this study simulated four possible scenarios. Among them, under the HDS scenario, construction land expanded by 21,758.77 km^2 over 30 years, leading to the highest LUCE and ECS. The LCS scenario is the only scenario where carbon storage increases, mainly due to a significant increase in forests and water. Under the NS scenario, the growth rates of LUCE and ECS remain consistent with those from 2000 to 2020. Under the CPS scenario, carbon storage slowly decreased by a total of 2708.81 $\times$ 10^4 t, while carbon emissions increased by 15,162.37 $\times$ 10^4 t; the increase in emissions was only higher than that of the LCS scenario.

(3) Shandong Province faces significant emission reduction pressure but also possesses considerable carbon sequestration potential. Against the backdrop of carbon neutrality, it is essential for Shandong Province to implement precise control over regional LUCC and optimize existing land policies. For instance, it is crucial to delineate ecological protection zones and development exclusion zones while ensuring the preservation of arable land. Furthermore, proactive measures should be taken to expand major ecological protection areas, particularly by transitioning the planning of urban built-up areas from rapid expansion to intensification. Moreover, promoting integrated urban–rural development is imperative.

The research findings provide a new pathway for Shandong Province to actively promote carbon peak and carbon neutrality through land low-carbon management. By balancing the relationships among ecological protection, cropland preservation, and urban development, carbon balance can be facilitated in terrestrial ecosystems. Additionally, this study offers valuable insights for other regions to address climate issues through optimizing land use patterns.

Author Contributions: Conceptualization, W.Q.; methodology, X.-Y.M., W.-J.L. and Y.-F.X.; software, X.-Y.M.; validation, X.-Y.M.; formal analysis, X.-Y.M.; resources, W.Q.; data curation, X.-Y.M.; writing—original draft, X.-Y.M.; writing—review and editing, X.-Y.M., W.Q. and Q.S.; visualization, X.-Y.M. and W.Q.; supervision, W.Q.; project administration, W.Q. and Q.S. All authors have read and agreed to the published version of the manuscript.

Funding: This research received no external funding.

Institutional Review Board Statement: Not applicable.

Informed Consent Statement: Not applicable.

Data Availability Statement: Related data are available upon reasonable request.

Conflicts of Interest: The authors declare no conflicts of interest.

References

1. Wang, Y.; Guo, C.-H.; Chen, X.-J.; Jia, L.-Q.; Guo, X.-N.; Chen, R.-S.; Zhang, M.-S.; Chen, Z.-Y.; Wang, H.-D. Carbon peak and carbon neutrality in China: Goals, implementation path and prospects. *China Geol.* **2021**, *4*, 720–746. [CrossRef]
2. Den Elzen, M.; Fekete, H.; Höhne, N.; Admiraal, A.; Forsell, N.; Hof, A.F.; Olivier, J.G.; Roelfsema, M.; van Soest, H. Greenhouse gas emissions from current and enhanced policies of China until 2030: Can emissions peak before 2030? *Energy Policy* **2016**, *89*, 224–236. [CrossRef]
3. Hong, C.; Burney, J.A.; Pongratz, J.; Nabel, J.E.; Mueller, N.D.; Jackson, R.B.; Davis, S.J. Global and regional drivers of land-use emissions in 1961–2017. *Nature* **2021**, *589*, 554–561. [CrossRef] [PubMed]
4. Normile, D. China's bold climate pledge earns praise—But is it feasible? *Science* **2020**, *370*, 17–18. [CrossRef]
5. Tay, A. By the numbers: China's net-zero ambitions. *Nature* **2022**. [CrossRef] [PubMed]
6. Zhong, C.; Guo, H.; Swan, I.; Gao, P.; Yao, Q.; Li, H. Evaluating trends, profits, and risks of global cities in recent urban expansion for advancing sustainable development. *Habitat Int.* **2023**, *138*, 102869. [CrossRef]
7. Jones, C.D.; Askew, A.J. Emissions scenarios and targets aligned to meet climate goals. *Nature* **2023**, *624*, 46–48. [CrossRef]

8. Liu, M.; Chen, Y.; Chen, K.; Chen, Y. Progress and Hotspots of Research on Land-Use Carbon Emissions: A Global Perspective. *Sustainability* **2023**, *15*, 7245. [CrossRef]
9. Wu, Z.; Huang, X.; Chen, R.; Mao, X.; Qi, X. The United States and China on the paths and policies to carbon neutrality. *J. Environ. Manag.* **2022**, *320*, 115785. [CrossRef]
10. Zhang, H.; Gu, P.; Cao, G.; He, D.; Cai, B. The Impact of Land-Use Structure on Carbon Emission in China. *Sustainability* **2023**, *15*, 2398. [CrossRef]
11. Gao, J.; Zhang, W.; Yang, C.; Wang, Q.; Yuan, R.; Wang, R.; Zhang, L.; Li, Z.; Luo, X. A Comparative Study of China's Carbon Neutrality Policy and International Research Keywords under the Background of Decarbonization Plans in China. *Sustainability* **2023**, *15*, 13069. [CrossRef]
12. Lai, L.; Huang, X.; Yang, H.; Chuai, X.; Zhang, M.; Zhong, T.; Chen, Z.; Chen, Y.; Wang, X.; Thompson, J.R. Carbon emissions from land-use change and management in China between 1990 and 2010. *Sci. Adv.* **2016**, *2*, e1601063. [CrossRef] [PubMed]
13. Wang, N.; Chen, X.; Zhang, Z.; Pang, J. Spatiotemporal dynamics and driving factors of county-level carbon storage in the Loess Plateau: A case study in Qingcheng County, China. *Ecol. Indic.* **2022**, *144*, 109460. [CrossRef]
14. Yin, C.; Zhao, W.; Ye, J.; Muroki, M.; Pereira, P. Ecosystem carbon sequestration service supports the Sustainable Development Goals progress. *J. Environ. Manag.* **2023**, *330*, 117155. [CrossRef] [PubMed]
15. Ke, N.; Lu, X.; Zhang, X.; Kuang, B.; Zhang, Y. Urban land use carbon emission intensity in China under the "double carbon" targets: Spatiotemporal patterns and evolution trend. *Environ. Sci. Pollut. Res.* **2023**, *30*, 18213–18226. [CrossRef] [PubMed]
16. Zhao, L.; Yang, C.-H.; Zhao, Y.-C.; Wang, Q.; Zhang, Q.-P. Spatial Correlations of Land Use Carbon Emissions in Shandong Peninsula Urban Agglomeration: A Perspective from City Level Using Remote Sensing Data. *Remote Sens.* **2023**, *15*, 1488. [CrossRef]
17. Li, X.; Liu, Z.; Li, S.; Li, Y.; Wang, W. Urban Land Carbon Emission and Carbon Emission Intensity Prediction Based on Patch-Generating Land Use Simulation Model and Grid with Multiple Scenarios in Tianjin. *Land* **2023**, *12*, 2160. [CrossRef]
18. Zhang, Z.; Yu, X.; Hou, Y.; Chen, T.; Lu, Y.; Sun, H. Carbon Emission Patterns and Carbon Balance Zoning in Urban Territorial Spaces Based on Multisource Data: A Case Study of Suzhou City, China. *ISPRS Int. J. Geo-Inf.* **2023**, *12*, 385. [CrossRef]
19. Zhong, J.-L.; Qi, W.; Dong, M.; Xu, M.-H.; Zhang, J.-Y.; Xu, Y.-X.; Zhou, Z.-J. Land Use Carbon Emission Measurement and Risk Zoning under the Background of the Carbon Peak: A Case Study of Shandong Province, China. *Sustainability* **2022**, *14*, 15130. [CrossRef]
20. Zhan, J.; Wang, C.; Wang, H.; Zhang, F.; Li, Z. Pathways to achieve carbon emission peak and carbon neutrality by 2060: A case study in the Beijing-Tianjin-Hebei region, China. *Renew. Sustain. Energy Rev.* **2024**, *189*, 113955. [CrossRef]
21. Li, L.; Huang, X.; Yang, H. Optimizing land use patterns to improve the contribution of land use planning to carbon neutrality target. *Land Use Policy* **2023**, *135*, 106959. [CrossRef]
22. Fang, Z.; Ding, T.; Chen, J.; Xue, S.; Zhou, Q.; Wang, Y.; Wang, Y.; Huang, Z.; Yang, S. Impacts of land use/land cover changes on ecosystem services in ecologically fragile regions. *Sci. Total Environ.* **2022**, *831*, 154967. [CrossRef] [PubMed]
23. Nath, B.; Wang, Z.; Ge, Y.; Islam, K.; Singh, R.P.; Niu, Z. Land Use and Land Cover Change Modeling and Future Potential Landscape Risk Assessment Using Markov-CA Model and Analytical Hierarchy Process. *ISPRS Int. J. Geo-Inf.* **2020**, *9*, 134. [CrossRef]
24. Shao, Z.; Chen, C.; Liu, Y.; Cao, J.; Liao, G.; Lin, Z. Impact of Land Use Change on Carbon Storage Based on FLUS-InVEST Model: A Case Study of Chengdu–Chongqing Urban Agglomeration, China. *Land* **2023**, *12*, 1531. [CrossRef]
25. Luo, G.; Yin, C.; Chen, X.; Xu, W.; Lu, L. Combining system dynamic model and CLUE-S model to improve land use scenario analyses at regional scale: A case study of Sangong watershed in Xinjiang, China. *Ecol. Complex.* **2010**, *7*, 198–207. [CrossRef]
26. Liang, X.; Guan, Q.; Clarke, K.C.; Liu, S.; Wang, B.; Yao, Y. Understanding the drivers of sustainable land expansion using a patch-generating land use simulation (PLUS) model: A case study in Wuhan, China. *Comput. Environ. Urban Syst.* **2021**, *85*, 101569. [CrossRef]
27. Wei, X.; Zhang, S.; Luo, P.; Zhang, S.; Wang, H.; Kong, D.; Zhang, Y.; Tang, Y.; Sun, S. A Multi-Scenario Prediction and Spatiotemporal Analysis of the Land Use and Carbon Storage Response in Shaanxi. *Remote Sens.* **2023**, *15*, 5036. [CrossRef]
28. Zhang, J.; Zhang, C.; Dong, H.; Zhang, L.; He, S. Spatial–Temporal Change Analysis and Multi-Scenario Simulation Prediction of Land-Use Carbon Emissions in the Wuhan Urban Agglomeration, China. *Sustainability* **2023**, *15*, 11021. [CrossRef]
29. Wang, K.; Li, X.; Lyu, X.; Dang, D.; Dou, H.; Li, M.; Liu, S.; Cao, W. Optimizing the Land Use and Land Cover Pattern to Increase Its Contribution to Carbon Neutrality. *Remote Sens.* **2022**, *14*, 4751. [CrossRef]
30. Ma, S.; He, L.; Fang, Y.; Liu, X.; Fan, Y.; Wang, S. Intensive land management through policy intervention and spatiotemporal optimization can achieve carbon neutrality in advance. *J. Clean. Prod.* **2023**, *385*, 135635. [CrossRef]
31. Zhang, S.; Yang, P.; Xia, J.; Wang, W.; Cai, W.; Chen, N.; Hu, S.; Luo, X.; Li, J.; Zhan, C. Land use/land cover prediction and analysis of the middle reaches of the Yangtze River under different scenarios. *Sci. Total Environ.* **2022**, *833*, 155238. [CrossRef] [PubMed]
32. Li, J.; Chunyu, X.; Huang, F. Land Use Pattern Changes and the Driving Forces in the Shiyang River Basin from 2000 to 2018. *Sustainability* **2023**, *15*, 154. [CrossRef]
33. Zhang, C.-Y.; Zhao, L.; Zhang, H.; Chen, M.-N.; Fang, R.-Y.; Yao, Y.; Zhang, Q.-P.; Wang, Q. Spatial-temporal characteristics of carbon emissions from land use change in Yellow River Delta region, China. *Ecol. Indic.* **2022**, *136*, 108623. [CrossRef]

34. Rong, T.; Zhang, P.; Zhu, H.; Jiang, L.; Li, Y.; Liu, Z. Spatial correlation evolution and prediction scenario of land use carbon emissions in China. *Ecol. Inform.* **2022**, *71*, 101802. [CrossRef]
35. Wu, Z.; Zhou, L.; Wang, Y. Prediction of the Spatial Pattern of Carbon Emissions Based on Simulation of Land Use Change under Different Scenarios. *Land* **2022**, *11*, 1788. [CrossRef]
36. Fu, Y.; Huang, M.; Gong, D.; Lin, H.; Fan, Y.; Du, W. Dynamic Simulation and Prediction of Carbon Storage Based on Land Use/Land Cover Change from 2000 to 2040: A Case Study of the Nanchang Urban Agglomeration. *Remote Sens.* **2023**, *15*, 4645. [CrossRef]
37. Noon, M.L.; Goldstein, A.; Ledezma, J.C.; Roehrdanz, P.R.; Cook-Patton, S.C.; Spawn-Lee, S.A.; Wright, T.M.; Gonzalez-Roglich, M.; Hole, D.G.; Rockström, J. Mapping the irrecoverable carbon in Earth's ecosystems. *Nat. Sustain.* **2022**, *5*, 37–46. [CrossRef]
38. Ren, Q.; Liu, D.; Liu, Y. Spatio-temporal variation of ecosystem services and the response to urbanization: Evidence based on Shandong province of China. *Ecol. Indic.* **2023**, *151*, 110333. [CrossRef]
39. Lu, L.; Xue, Q.; Zhang, X.; Qin, C.; Jia, L. Spatiotemporal Variation and Quantitative Attribution of Carbon Storage Based on Multiple Satellite Data and a Coupled Model for Jinan City, China. *Remote Sens.* **2023**, *15*, 4472. [CrossRef]
40. Tien, T.-L. A research on the grey prediction model GM(1, n). *Appl. Math. Comput.* **2012**, *218*, 4903–4916. [CrossRef]
41. Tian, L.; Tao, Y.; Fu, W.; Li, T.; Ren, F.; Li, M. Dynamic Simulation of Land Use/Cover Change and Assessment of Forest Ecosystem Carbon Storage under Climate Change Scenarios in Guangdong Province, China. *Remote Sens.* **2022**, *14*, 2330. [CrossRef]
42. Wang, Y.; Fan, H.; Wang, H.; Che, Y.; Wang, J.; Liao, Y.; Lv, S. High-carbon expansion or low-carbon intensive and mixed land-use? Recent observations from megacities in developing countries: A case study of Shanghai, China. *J. Environ. Manag.* **2023**, *348*, 119294. [CrossRef] [PubMed]
43. Huang, M.-T.; Zhai, P.-M. Achieving Paris Agreement temperature goals requires carbon neutrality by middle century with far-reaching transitions in the whole society. *Adv. Clim. Change Res.* **2021**, *12*, 281–286. [CrossRef]
44. Zhu, G.; Qiu, D.; Zhang, Z.; Sang, L.; Liu, Y.; Wang, L.; Zhao, K.; Ma, H.; Xu, Y.; Wan, Q. Land-use changes lead to a decrease in carbon storage in arid region, China. *Ecol. Indic.* **2021**, *127*, 107770. [CrossRef]
45. Wang, J.; Zhang, J.; Xiong, N.; Liang, B.; Wang, Z.; Cressey, E.L. Spatial and Temporal Variation, Simulation and Prediction of Land Use in Ecological Conservation Area of Western Beijing. *Remote Sens.* **2022**, *14*, 1452. [CrossRef]
46. Yu, R.; Cheng, H.; Ye, Y.; Wang, Q.; Fan, S.; Li, T.; Wang, C.; Su, Y.; Zhang, X. Optimization of the Territorial Spatial Patterns Based on MOP and PLUS Models: A Case Study from Hefei City, China. *Int. J. Environ. Res. Public Health* **2023**, *20*, 1804. [CrossRef]
47. Zhu, E.; Deng, J.; Zhou, M.; Gan, M.; Jiang, R.; Wang, K.; Shahtahmassebi, A. Carbon emissions induced by land-use and land-cover change from 1970 to 2010 in Zhejiang, China. *Sci. Total Environ.* **2019**, *646*, 930–939. [CrossRef] [PubMed]
48. Cui, X.; Wei, X.; Liu, W.; Zhang, F.; Li, Z. Spatial and temporal analysis of carbon sources and sinks through land use/cover changes in the Beijing-Tianjin-Hebei urban agglomeration region. *Phys. Chem. Earth Parts A/B/C* **2019**, *110*, 61–70. [CrossRef]
49. Wang, Z.; Li, X.; Mao, Y.; Li, L.; Wang, X.; Lin, Q. Dynamic simulation of land use change and assessment of carbon storage based on climate change scenarios at the city level: A case study of Bortala, China. *Ecol. Indic.* **2022**, *134*, 108499. [CrossRef]
50. Liu, H.; Nie, J.; Cai, B.; Cao, L.; Wu, P.; Pang, L.; Wang, X. CO_2 emissions patterns of 26 cities in the Yangtze River Delta in 2015: Evidence and implications. *Environ. Pollut.* **2019**, *252*, 1678–1686. [CrossRef]
51. Yu, G.; Liu, T.; Wang, Q.; Li, T.; Li, X.; Song, G.; Feng, Y. Impact of Land Use/Land Cover Change on Ecological Quality during Urbanization in the Lower Yellow River Basin: A Case Study of Jinan City. *Remote Sens.* **2022**, *14*, 6273. [CrossRef]
52. Williams, K. Urban intensification policies in England: Problems and contradictions. *Land Use Policy* **1999**, *16*, 167–178. [CrossRef]
53. Yin, X.; Chen, J.; Li, J. Rural innovation system: Revitalize the countryside for a sustainable development. *J. Rural Stud.* **2022**, *93*, 471–478. [CrossRef]
54. Rajput, S.; Singh, S.P. Industry 4.0 Model for circular economy and cleaner production. *J. Clean. Prod.* **2020**, *277*, 123853. [CrossRef]
55. Ren, F.; Misselbrook, T.; Sun, N.; Zhang, X.; Zhang, S.; Jiao, J.; Xu, M.; Wu, L. Spatial changes and driving variables of topsoil organic carbon stocks in Chinese croplands under different fertilization strategies. *Sci. Total Environ.* **2021**, *767*, 144350. [CrossRef] [PubMed]
56. Shen, X.; Wang, L.; Wu, C.; Lv, T.; Lu, Z.; Luo, W.; Li, G. Local interests or centralized targets? How China's local government implements the farmland policy of Requisition–Compensation Balance. *Land Use Policy* **2017**, *67*, 716–724. [CrossRef]
57. Yang, Y.; Li, H.; Qian, C. Analysis of the implementation effects of ecological restoration projects based on carbon storage and eco-environmental quality: A case study of the Yellow River Delta, China. *J. Environ. Manag.* **2023**, *340*, 117929. [CrossRef] [PubMed]
58. Mohanta, M.R.; Mohanta, A.; Mohapatra, U.; Mohanty, R.C.; Sahu, S.C. Carbon stock assessment and its relation with tree biodiversity in Tropical Moist Deciduous Forest of Similipal Biosphere Reserve, Odisha, India. *Trop. Ecol.* **2020**, *61*, 497–508. [CrossRef]
59. Zhai, T.; Wang, J.; Fang, Y.; Huang, L.; Liu, J.; Zhao, C. Integrating Ecosystem Services Supply, Demand and Flow in Ecological Compensation: A Case Study of Carbon Sequestration Services. *Sustainability* **2021**, *13*, 1668. [CrossRef]

60. Salunkhe, O.; Khare, P.; Kumari, R.; Khan, M. A systematic review on the aboveground biomass and carbon stocks of Indian forest ecosystems. *Ecol. Process.* **2018**, *7*, 17. [CrossRef]
61. Ying, Z.; Xiaoge, L.; Yali, W. Forest carbon sequestration potential in China under the background of carbon emission peak and carbon neutralization. *J. Beijing For. Univ.* **2022**, *44*, 38–47. [CrossRef]